

## Local Reaction Environments and their Properties for Ethene Deuteration on the Surfaces of SMSI† Catalysts

Hideaki Yoshitake, Kiyotaka Asakura and Yasuhiro Iwasawa\*

*Department of Chemistry, Faculty of Science, The University of Tokyo, Hongo, Bunkyo-ku, Tokyo 113, Japan*

Ethene deuteration and H<sub>2</sub>-D<sub>2</sub> exchange reaction over Nb<sub>2</sub>O<sub>5</sub>-supported Rh and Ir catalysts have been investigated in relation to strong metal-support interaction (SMSI) phenomena. The activation energies for these reactions were considerably changed by high-temperature reduction of the catalyst in the case of Ir/Nb<sub>2</sub>O<sub>5</sub>, but were not modified in the case of Rh/Nb<sub>2</sub>O<sub>5</sub>. The change is ascribed to a reduction in the energy barrier for deuterium dissociation. The deuterium distribution in ethane formed during ethene deuteration was also investigated at various reaction temperatures and as a function of the reduction time of the catalyst. By studying the catalysts in their working state instead of by static adsorption measurements two kinds of active sites in different environments are suggested to exist on the surface of these catalysts in the SMSI states. One of these sites (site I) is on the bare metal surface and the other (site II) is on the perimeter of a migrating NbO<sub>x</sub> island. The surface isotopic ratio of hydrogen during ethene deuteration is different at sites I and II. Site I, on which D<sub>2</sub> dissociates, acts as a deuterium supply for site II. A model for the deuteration of ethene on the SMSI catalysts is proposed.

Catalysis by noble metals supported on TiO<sub>2</sub> or Nb<sub>2</sub>O<sub>5</sub> has attracted considerable interest in relation to strong metal-support interaction (SMSI) phenomena as well as surface chemistry, in order to inspect physicochemical properties controlling metal catalysis.<sup>1,2</sup> Numerous authors have pointed out the characteristic features of SMSI states of catalysts, such as a reduction in the hydrogenation activity for alkenes,<sup>3,4</sup> a drastic decrease in hydrogenolysis activity<sup>4,5</sup> and a unique product distribution in CO hydrogenation.<sup>6,7</sup> These changes or modifications in catalysis are believed to derive from the presence of TiO<sub>x</sub> or NbO<sub>x</sub> that has migrated onto the metal surface, and hence SMSI catalysis is thought to be due to a blockage by TiO<sub>x</sub> or NbO<sub>x</sub> on the metal surface,<sup>5,8–12</sup> the destruction of the ensemble required for activity,<sup>5</sup> or an adsorbate-Ti<sup>n+</sup> interaction in the periphery of migrated TiO<sub>x</sub>, which is assumed to be an important intermediate for enhanced hydrogenation.<sup>13–15</sup>

Catalytic reactions are generally composed of several surface processes (such as adsorption or desorption, the diffusion/transport of adsorbates, and surface reactions in which more than one adsorbed species participate) which are affected by the structures and environments at the surface in a different manner. Catalysis by SMSI catalysts therefore includes the interaction between active site and reaction intermediates, the relationship between surface processes and specific structures and environments on the metal surfaces brought about by TiO<sub>x</sub> or NbO<sub>x</sub>.

These physical and chemical (electronic) factors are likely to be common among metal catalyses involving promoters. A study of catalysis by SMSI catalysts showing characteristic features may provide a deeper understanding of the essential factors involved in metal catalysis and the reaction environments on metal surfaces, in addition

† Strong metal-support interaction.

to information on the development of active multifunctional metal catalysts. In the present paper we report an investigation of the role of  $\text{NbO}_x$  species in ethene deuteration on  $\text{Ir}/\text{Nb}_2\text{O}_5$  and  $\text{Rh}/\text{Nb}_2\text{O}_5$  which shows that  $\text{NbO}_x$  diffused onto the metal surface brings about not only a modification of the stability of the reaction intermediates but also a differentiation between two reaction environments with different local ratios of hydrogen and deuterium atoms.

## Experimental

Supported rhodium and iridium catalysts were prepared by conventional impregnation of  $\text{Nb}_2\text{O}_5$  (Wako Pure Chemical Industries Ltd, 99.9%) with an aqueous solution of  $\text{RhCl}_3 \cdot 3\text{H}_2\text{O}$  or  $\text{IrCl}_3 \cdot 1.5\text{H}_2\text{O}$  (Soekawa Chemical Co., Ltd) followed by drying for 3 h at 393 K and calcination for 2 h at 773 K. The metal loadings were 2.0 and 2.4 wt % for  $\text{Rh}/\text{Nb}_2\text{O}_5$  and  $\text{Ir}/\text{Nb}_2\text{O}_5$ , respectively. The catalysts were pretreated with oxygen for 1 h at 673 K, followed by evacuation for 30 min, and reduced for 1 h at 433 K [for the low-temperature reduced (LTR) catalyst] or at 773 K [for the high-temperature reduced (HTR) catalyst], followed by evacuation for 30 min *in situ* before each catalytic reaction. The particle sizes of the supported metals were estimated by hydrogen chemisorption at room temperature, transmission electron microscopy (TEM) and X-ray diffraction (X.r.d.). No surface chloride was detected by X.p.s. on the reduced catalyst.

Ethene, purchased from Takachiho Trading Co., Ltd (99.9%), was purified by freeze-thaw cycles. Hydrogen and deuterium gases of research grade were further purified through a molecular-sieve trap at 77 K.

The reactions of  $\text{D}_2$  with ethene,  $\text{H}_2$  with ethene and a  $\text{D}_2$ - $\text{H}_2$  mixture with ethene were carried out in a closed circulating system (dead volume  $150\text{ cm}^3$ ) in the temperature range 210–321 K. A small portion of the reaction gas during the reaction was analysed at intervals by gas chromatography using a VZ-10 column. Deuteration products in the  $\text{D}_2$ -ethene reaction were also analysed by mass spectrometry with ULVAC MSQ-150A after separation with VZ-10 column. Isotope effects in the fragmentation of C—H and C—D were negligible.

## Results and Discussion

### Kinetic Behaviour

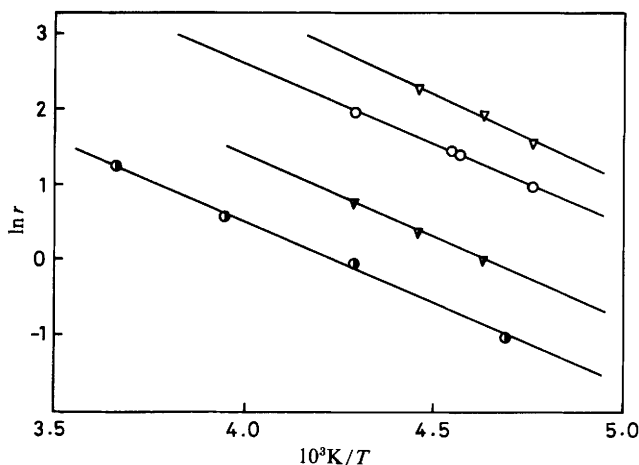
The average particle sizes of the catalysts determined by  $\text{H}_2$  chemisorption, TEM and X.r.d. are shown in table 1. The  $H/M$  values of HTR for both  $\text{Rh}/\text{Nb}_2\text{O}_5$  and  $\text{Ir}/\text{Nb}_2\text{O}_5$  were almost zero compared with those for LTR catalysts, owing to SMSI phenomena. Except for this, all values are in good agreement when a 1:1 stoichiometry for H/Rh or H/Ir and a spherical shape were assumed in determining particle sizes by  $\text{H}_2$  chemisorption. Significant differences between LTR and HTR catalysts were not found in the TEM and X.r.d. results, which suggests that metal particle sizes were not altered significantly by high-temperature reduction.

Fig. 1 shows Arrhenius plots for total ethane formation in the  $\text{D}_2$ -ethene reaction and for HD formation in the  $\text{D}_2$ - $\text{H}_2$ -ethene reaction on  $\text{Rh}/\text{Nb}_2\text{O}_5$ . The rates on the LTR catalyst,  $d[\text{ethane}]/dt$  or  $d[\text{HD}]/dt$ , are normalized by the  $H/M$  value to show the turnover frequencies (the activity of each surface Rh atom) in fig. 1, where the rates for the HTR catalyst are also normalized to show the activity on the same scale as that of the LTR catalyst; this avoids the large error derived from the division of the observed rates by the very small  $H/M$  value for HTR. When the rate of ethane formation is compared with that of HD formation, the latter should be reduced to half. The activation energy for HD formation ( $17\text{ kJ mol}^{-1}$ ) on the LTR catalyst was almost the same as that for ethane formation ( $16\text{ kJ mol}^{-1}$ ). These values were also similar to those for the HTR

**Table 1.** Estimation of average particle size (nm)

catalyst		$H/M^a$	TEM	X.r.d.
Rh/Nb <sub>2</sub> O <sub>5</sub>	LTR	10 (0.11)	9.8	9.3
	HTR	— (0.01)	10.2	9.6
Ir/Nb <sub>2</sub> O <sub>5</sub>	LTR	4 (0.31)	4.2	4.2
	HTR	— (0.00)	4.4	4.1

<sup>a</sup> The particle sizes, calculated from  $H/M$  values are given in parentheses.



**Fig. 1.** Arrhenius plots for ethane formation in the D<sub>2</sub>-ethene reaction [ $p(\text{D}_2) = p(\text{CH}_2=\text{CH}_2) = 1.1 \text{ kPa}$ ] and HD formation in the H<sub>2</sub>-D<sub>2</sub>-ethene reaction [ $p(\text{H}_2) = p(\text{D}_2) = p(\text{CH}_2=\text{CH}_2)/2 = 0.53 \text{ kPa}$ ] on Rh/Nb<sub>2</sub>O<sub>5</sub>: ○, ethane formation on the LTR catalyst; ▽, HD formation on the LTR catalyst; ●, ethane formation on the HTR catalyst; ▼, HD formation on the HTR catalyst. The rates,  $d[\text{ethane}]/dt$  and  $d[\text{HD}]/dt$ , were normalized by the  $H/M$  value for the LTR catalyst.

catalyst (17 and 17 kJ mol<sup>-1</sup>, respectively). In contrast, on the Ir/Nb<sub>2</sub>O<sub>5</sub> HTR the activation energies for both ethane and HD formation, 3 and 2 kJ mol<sup>-1</sup>, respectively, were much smaller than those for the Ir/Nb<sub>2</sub>O<sub>5</sub> LTR, 22 and 23 kJ mol<sup>-1</sup>, respectively, as shown in fig. 2(a) and (b). The activation energies, 19 and 0 kJ mol<sup>-1</sup>, for ethane formation in the H<sub>2</sub>-ethene reaction on the LTR and HTR catalysts, respectively, were a little smaller than those for ethane formation in the D<sub>2</sub>-ethene reaction. The activation energies for HD and ethane formation were almost the same as on Rh/Nb<sub>2</sub>O<sub>5</sub>, as shown in fig. 2.

The Horiuti-Polanyi mechanism has been widely accepted to describe ethene hydrogenation over noble metals; it includes the associative adsorption of ethene, its transformation to half-hydrogenated ethyl species by the reaction with a hydrogen atom on surface and the hydrogenation step to form ethane. The rate-determining step in this mechanism is the dissociation of hydrogen at relatively low temperatures or the addition of a second hydrogen atom to the half-hydrogenated species at higher temperatures. The activation energy for the former step is positive, while that in the latter case is often negative. There is consequently an optimum temperature for the rate of ethane formation.<sup>16</sup>

The rate-determining step in ethene deuteration under the present experimental

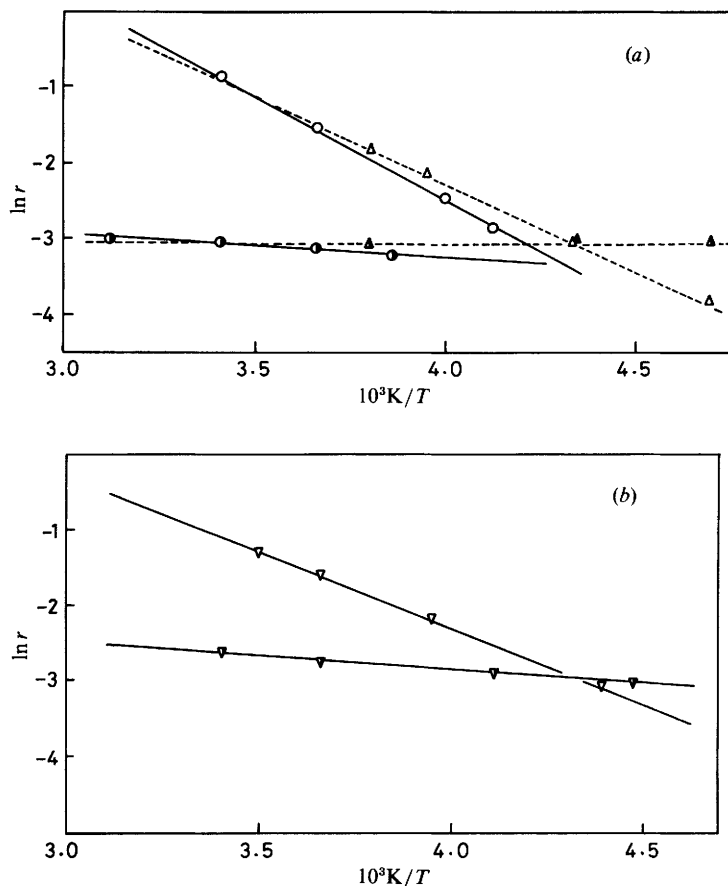


**Fig. 2.** (a) Arrhenius plots for ethane formation in deuteration and hydrogenation of ethene on Ir/Nb<sub>2</sub>O<sub>5</sub>; ○, D<sub>2</sub>-ethene reaction on the LTR catalyst; ●, D<sub>2</sub>-ethene reaction on the HTR catalyst; △, H<sub>2</sub>-ethene reaction on the LTR catalyst; ▲, H<sub>2</sub>-ethene reaction on the HTR catalyst. The rates were normalized by the  $H/M$  value for the LTR catalyst.  $p(\text{D}_2) = p(\text{H}_2) = p(\text{CH}_2=\text{CH}_2) = 1.1$  kPa. (b) Arrhenius plots for HD formation in the H<sub>2</sub>-D<sub>2</sub>-ethene reaction on Ir/Nb<sub>2</sub>O<sub>5</sub>: ▽, LTR; ▾, HTR. The rates were normalized by the  $H/M$  value for the LTR catalyst.  $p(\text{D}_2) = p(\text{H}_2) = (\frac{1}{2})p(\text{CH}_2=\text{CH}_2) = 0.53$  kPa.

conditions is suggested to be the dissociation of D<sub>2</sub>, because the activation energy for ethane formation agrees well with that of HD formation, as shown in fig. 1 and 2. This holds true for both LTR and HTR catalysts. There is an isotopic effect observed in ethane formation in fig. 2, which may be ascribed to the difference between H<sub>2</sub> and D<sub>2</sub> in the energy barrier for the dissociation.

The difference in the activation energies for LTR and HTR Ir/Nb<sub>2</sub>O<sub>5</sub> observed in fig. 2 suggests a large modification of the electronic state of the metal surface by SMSI. In contrast, a change in activation energy was not observed with Rh/Nb<sub>2</sub>O<sub>5</sub> in fig. 1, where the SMSI phenomenon with the suppression of reaction rates appears as 'site-blocking' by inactive migrated species in this system.

The difference observed between Ir and Rh may arise from the difference in their particle sizes, or more likely in the strength and morphologic features of their SMSI. Similar differences in SMSI phenomena between different metals has been reported in benzene hydrogenation on Rh/TiO<sub>2</sub> and Pt/TiO<sub>2</sub>.<sup>3</sup>

The catalytic activity of the HTR Ir/Nb<sub>2</sub>O<sub>5</sub> catalyst was higher than that of the LTR catalyst for ethane hydrogenation and H<sub>2</sub>-D<sub>2</sub> exchange at lower temperatures, in spite of the large decrease in the number of active Ir sites estimated from the *H/M* value. In other words, the Ir sites for hydrogen dissociation are activated by NbO<sub>x</sub> that has migrated onto the Ir metal surface in the SMSI state.

### Deuteroethane Distribution

The deuterium distributions (relative amounts) in deuteroethane produced at the initial stage of the D<sub>2</sub>-ethene reaction are summarized in tables 2 and 3. On Rh/Nb<sub>2</sub>O<sub>5</sub> the order of population was <sup>2</sup>H<sub>2</sub> > <sup>2</sup>H<sub>1</sub> ≥ <sup>2</sup>H<sub>0</sub> for the LTR catalyst, whereas the order <sup>2</sup>H<sub>0</sub>, <sup>2</sup>H<sub>2</sub> > <sup>2</sup>H<sub>1</sub> was observed for the HTR catalyst. Also, in the case of Ir/Nb<sub>2</sub>O<sub>5</sub> the population of deuteroethane formed was in the order <sup>2</sup>H<sub>2</sub> > <sup>2</sup>H<sub>1</sub> > <sup>2</sup>H<sub>0</sub> for the LTR catalyst but <sup>2</sup>H<sub>0</sub>, <sup>2</sup>H<sub>2</sub> > <sup>2</sup>H<sub>1</sub> for the HTR catalyst. As a whole, the trend of the SMSI effect on the distribution of deuteroethane was the same for Rh/Nb<sub>2</sub>O<sub>5</sub> and Ir/Nb<sub>2</sub>O<sub>5</sub>.

The compositions of H<sub>2</sub>, HD and D<sub>2</sub> in the gas phase in the initial stage of the D<sub>2</sub>-ethene reaction on Rh/Nb<sub>2</sub>O<sub>5</sub> and Ir/Nb<sub>2</sub>O<sub>5</sub> are given in tables 2 and 3. These results demonstrate that the change in the deuterium population of ethane on the LTR and HTR catalysts is not derived from the isotopic compositions of hydrogen in the gas phase during the deuteration of ethene. Again, very small amounts of deuteroethene as compared with deuteroethane formation were observed in the gas phase.

The distribution of deuteroethane reflects the stability of the half-hydrogenated intermediate of ethane deuteration. The population must be ordered, with <sup>2</sup>H<sub>2</sub> > <sup>2</sup>H<sub>1</sub> > <sup>2</sup>H<sub>0</sub> or <sup>2</sup>H<sub>0</sub> > <sup>2</sup>H<sub>1</sub> > <sup>2</sup>H<sub>2</sub>, if the reaction occurs on only one type of active site with uniform reaction environments.<sup>17,18</sup> In fact, Rh/Al<sub>2</sub>O<sub>3</sub> and Ir/Al<sub>2</sub>O<sub>3</sub> have been classified as a <sup>2</sup>H<sub>2</sub> > <sup>2</sup>H<sub>1</sub> > <sup>2</sup>H<sub>0</sub> group at the reaction temperatures where the rate-determining step is the dissociation of hydrogen (as in the present conditions).<sup>19,20</sup> Our results for the LTR catalyst agreed with those for Rh/Al<sub>2</sub>O<sub>3</sub> and Ir/Al<sub>2</sub>O<sub>3</sub>, whereas the results for the HTR catalyst showed singular distributions, suggesting that ethane is formed on at least two different kinds of sites; one site may be preferable for the formation of [<sup>2</sup>H<sub>2</sub>]ethane and the other site for the formation of [<sup>2</sup>H<sub>0</sub>]ethane. The latter sites were newly generated by the high-temperature prerduction, while the former sites exist originally on the metal surface and may be modified a little in the SMSI state.

The population of deuteroethane must also reflect the populations of hydrogen and deuterium atoms on the metal surface. In order to obtain further information on this problem, the rates of the formation of each deuterogenated species in the D<sub>2</sub>-ethene reaction were examined as a function of the high-temperature pretreatment (reduction) time of Rh/Nb<sub>2</sub>O<sub>5</sub> (fig. 3). There was an optimum value for [<sup>2</sup>H<sub>0</sub>]ethane formation at *ca.* 50 min. The rate of [<sup>2</sup>H<sub>1</sub>]ethane formation also had a maximum at *ca.* 45 min reduction time, but the peak was smaller than that for [<sup>2</sup>H<sub>0</sub>]ethane formation. In the case of [<sup>2</sup>H<sub>2</sub>]ethane, the rate decreased monotonically with reduction, as shown in fig. 3. The slope of the curve for [<sup>2</sup>H<sub>0</sub>]ethane formation was more gentle than that for the [<sup>2</sup>H<sub>2</sub>]ethane formation, and consequently the reaction rates after the longer prerduction of catalyst were inverted, to form [<sup>2</sup>H<sub>0</sub>]ethane as a main product. Thus the presence of NbO<sub>x</sub> that has migrated onto the metal surfaces during the high-temperature reduction has a profound effect on the distribution of deuteroethane.

The rate of HD formation in the D<sub>2</sub>-H<sub>2</sub>-ethene reaction is also plotted as a function of the catalyst reduction time in fig. 3. In contrast to the deuterogenated ethanes, the curve for HD formation decreased monotonically, but convex downward. The values of *H/M* (the number of chemisorbed hydrogen atoms divided by the number of metal atoms included in the catalysts) are also plotted against reduction time in fig. 3. The curve for HD formation is similar to that for the *H/M* value in its dependence on the reduction time.



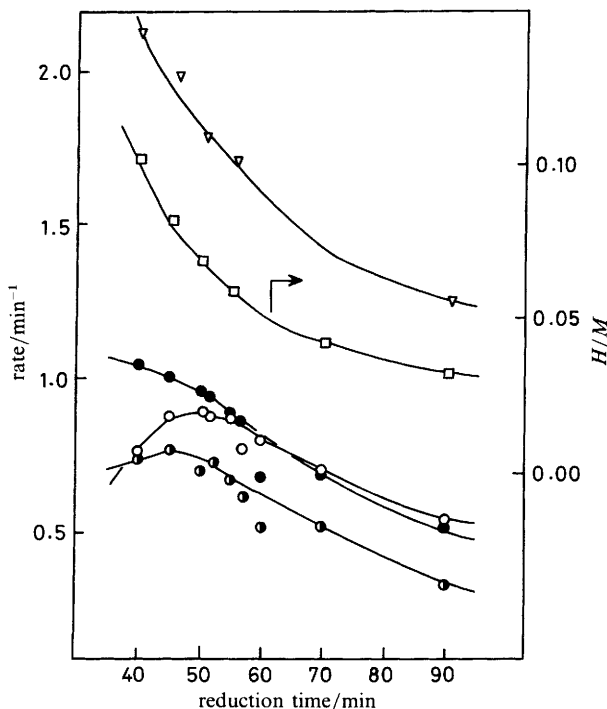


**Fig. 3.** Reaction rates for each deuterioethane and HD formation on Rh/Nb<sub>2</sub>O<sub>5</sub> and  $H/M$  values as a function of the high-temperature pretreatment (reduction) time of the catalyst: ○, [<sup>2</sup>H<sub>0</sub>]ethane; ●, [<sup>2</sup>H<sub>1</sub>]ethane; ●, [<sup>2</sup>H<sub>2</sub>]ethane; ▽, HD; □,  $H/M$ ; reaction temperature, 216 K; catalyst reduction temperature, 673 K;  $p(\text{D}_2) = p(\text{CH}_2=\text{CH}_2) = 1.1$  kPa for ethane formation,  $p(\text{H}_2) = p(\text{D}_2) = (\frac{1}{2})p(\text{CH}_2=\text{CH}_2) = 0.53$  kPa for HD formation.

Assuming that NbO<sub>x</sub> migrates onto the metal according to a diffusion process with self-similarity, the area of each environment can be written as a function of the high-temperature reduction time ( $t$ ) in the following equations:

$$\text{site I (on metal): } S_{\text{I}} = S_0 - \alpha t^{\frac{1}{2}} \quad (1)$$

$$\text{site II (periphery): } S_{\text{II}} = \beta t^{\frac{1}{2}} \quad (2)$$

$$\text{site III (on oxide): } S_{\text{III}} = \alpha t^{\frac{1}{2}} \quad (3)$$

where  $\alpha$  and  $\beta$  are constants and  $S_0$  is the initial area of the metal surface or the number of initial surface metal atoms. If the rate-determining step for ethene hydrogenation on the three reaction sites is the dissociation of hydrogen, the rate of ethene hydrogenation,  $r(t)$ , is expressed as a function of the reduction time as follows:

$$r(t) = \kappa_1(t)(S_0 - \alpha t^{\frac{1}{2}}) + \kappa_2(t)\beta t^{\frac{1}{2}} + \kappa_3(t)\alpha t^{\frac{1}{2}} \quad (4)$$

where  $\kappa_j(t)$  ( $j = 1, 2, 3$ ) represents the rate of the reaction occurring on site  $j$  per unit area (or per surface metal atom). The oxidation states of migrated Nb species have been suggested to be Nb<sup>2+</sup>, Nb<sup>3+</sup> or Nb<sup>4+</sup>.<sup>21</sup> However, it is difficult to characterize NbO<sub>x</sub> at the metal surface precisely in the present systems. Nevertheless, the ethene hydrogenation activities of the Nb<sup>+</sup> and Nb<sup>3+</sup> species supported on SiO<sub>2</sub> or TiO<sub>2</sub><sup>22</sup> were negligible under the present conditions, and the Nb<sup>5+</sup> monomer<sup>22</sup> and Nb<sub>2</sub>O<sub>5</sub> were inactive. Thus  $\kappa_1$ ,

$\kappa_2 \gg \kappa_3$  would be valid. If the value of  $\kappa_j(t)$  is approximately independent of the high-temperature reduction time under the present conditions, then eqn (4) is reduced to

$$r(t) = \kappa_1 S_0 + \kappa_2 \beta t^{\frac{1}{2}} - \kappa_1 \alpha t^{\frac{1}{2}} \quad (5)$$

Eqn (5) shows that  $r(t)$  has a maximum value if  $\kappa_2 \beta$  is significantly large compared with  $\kappa_1 \alpha$ . If the reaction proceeds on site I alone,  $\kappa_2 = 0$  and  $r(t)$  is equivalent to  $\kappa_1(S_0 - \alpha t^{\frac{1}{2}})$ , which is a downward-convex function.

With regard to ethene hydrogenation on Rh/Nb<sub>2</sub>O<sub>5</sub>, the SMSI treatment essentially changed neither the activation energy (fig. 1) nor the dependence of the rate on the partial pressures of ethene and hydrogen.<sup>23</sup> In this case the migrated NbO<sub>x</sub> only plays the role of 'site-blocker'. Thus eqn (5) can be applied to an analysis of the result of ethene deuteration on Rh/Nb<sub>2</sub>O<sub>5</sub>. The rate of HD formation in the H<sub>2</sub>-D<sub>2</sub>-ethene reaction on Rh/Nb<sub>2</sub>O<sub>5</sub> decreased with a downward curvature, like the value of  $H/M$  seen in fig. 3, which means that H<sub>2</sub>-D<sub>2</sub> exchange occurs only on site I; hence hydrogen dissociation is suggested to occur only on site I. In fig. 3 the migration of NbO<sub>x</sub> could be estimated to start at  $t = 40$  min, from the  $H/M$  value of 0.10 which agrees with that for the LTR catalyst.

By fitting eqn (5) to the experimental data of [<sup>2</sup>H<sub>0</sub>]-, [<sup>2</sup>H<sub>1</sub>]- and [<sup>2</sup>H<sub>2</sub>]ethane formation in fig. 3, we can obtain the parameters,  $\kappa_1 S_0$ ,  $\kappa_2 \beta$  and  $\kappa_1 \alpha$  for each type of deuterioethane. The results are given in table 4. The relative values for  $\kappa_1$  on site I and  $\kappa_2$  on site II were found to be <sup>2</sup>H<sub>0</sub>:<sup>2</sup>H<sub>1</sub>:<sup>2</sup>H<sub>2</sub> = 32:33:35 and <sup>2</sup>H<sub>0</sub>:<sup>2</sup>H<sub>1</sub>:<sup>2</sup>H<sub>2</sub> = 55:34:10, respectively. This demonstrates that the population of deuteration ethane formed on site I (the unmodified metal-surface area) is in the order <sup>2</sup>H<sub>2</sub> ≥ <sup>2</sup>H<sub>1</sub> ≥ <sup>2</sup>H<sub>0</sub>, and that on site II (newly generated at the periphery of NbO<sub>x</sub>) is in the order <sup>2</sup>H<sub>0</sub> > <sup>2</sup>H<sub>1</sub> > <sup>2</sup>H<sub>2</sub>. Values of  $\alpha/S_0$  were calculated from  $\kappa_1 \alpha$  and  $\kappa_1 S_0$  for [<sup>2</sup>H<sub>0</sub>]-, [<sup>2</sup>H<sub>1</sub>]- and [<sup>2</sup>H<sub>2</sub>]ethane in table 4. The values are in good agreement with 0.10 for  $\alpha/S_0$  calculated independently from the  $H/M$  curve in fig. 3.

In the case of Ir/Nb<sub>2</sub>O<sub>5</sub> eqn (4) cannot be applied unless the function  $\kappa_j(t)$  has been clarified by other techniques. The activation energy varies (fig. 2), and the rate of the reaction per unit area,  $\kappa_j(t)$ , must be explicitly represented as a function of reduction time. However, there will also be an optimum value for [<sup>2</sup>H<sub>0</sub>]ethane formation on Ir/Nb<sub>2</sub>O<sub>5</sub>.<sup>24</sup>

Recently Levin *et al.* reported a similar experiment for CO hydrogenation on TiO<sub>x</sub>/Rh.<sup>25</sup> In this case the activation energy for methanation varied in a complex manner in accordance with TiO<sub>x</sub> coverage, and  $\kappa_j(t)$  was not known. However, the methanation activity had an optimum value similar to our case.

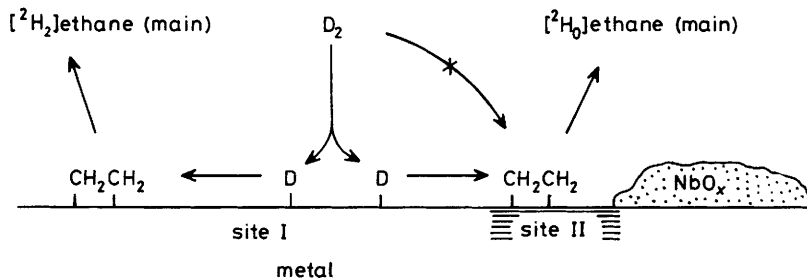
### Active Sites and Reaction Environments for Ethene Deuteration on SMSI Catalysts

While the static interaction of adsorbed species and surface structure has been extensively studied, there have been few studies which refer to the surface dynamic environments during catalysis, including the relationship between structures and isotopic concentrations at the surface.

As already discussed, there are two characteristic sites in ethene deuteration on SMSI catalysts. On site I, the bare metal surface, D<sub>2</sub> dissociates and ethene is associatively adsorbed, and on site II, the periphery of migrated NbO<sub>x</sub>, only ethene is adsorbed to interact with deuterium/hydrogen atoms transported from site I. Under the conditions for which D<sub>2</sub> dissociation is a slow step, the interconversion between associatively adsorbed ethene and half-hydrogenated species (and hence hydrogen exchange in ethene) readily occurs in order to dilute the deuterium on the surface. The surface isotopic ratio of deuterium concentration to hydrogen concentration may thus be different between site I and site II. The fact that [<sup>2</sup>H<sub>0</sub>]ethane was the predominant

**Table 4.** Fitting result of eqn (5)

	$\kappa_1 S_0/\text{min}^{-1}$	$\kappa_2 \beta/\text{min}^{-\frac{5}{2}}$	$\kappa_1 \alpha/\text{min}^{-\frac{3}{2}}$	$(\alpha/S_0)/\text{min}^{-\frac{1}{2}}$
[ $^2\text{H}_0$ ]ethane	0.77	0.21	0.081	0.105
[ $^2\text{H}_1$ ]ethane	0.74	0.13	0.085	0.115
[ $^2\text{H}_2$ ]ethane	1.05	0.04	0.091	0.087
HD	2.08	—	0.106	0.051
H/M	0.99	—	0.010	0.10

**Fig. 4.** Schematic model for the deuteration of ethene on SMSI catalysts.

product in the  $\text{D}_2$ -ethene reaction on site II in the SMSI catalyst indicates that the isotopic ratio (surface D/H) was significantly low at the  $\text{NbO}_x$  periphery. On the other hand, since [ $^2\text{H}_2$ ]ethane is main product on site I, the isotopic ratio (surface D/H) is considered to be large. In other words, the two sites are situated in different 'deuterium atmospheres' in the working state. Site I, on which  $\text{D}_2$  dissociates, acts as 'deuterium reserver' for site II in the SMSI state. A schematic model for ethene deuteration on  $\text{Rh}/\text{Nb}_2\text{O}_5$  in the SMSI state is shown in fig. 4. This model may also fit  $\text{Ir}/\text{Nb}_2\text{O}_5$  because of the similar phenomena shown in tables 2 and 3.<sup>24</sup>

The catalytic activity is controlled by the hydrogen-dissociation process, which is affected by both the number of sites and the electronic state of site I. There is no enhancement by SMSI for hydrogen dissociation on  $\text{Rh}/\text{Nb}_2\text{O}_5$ , while for  $\text{Ir}/\text{Nb}_2\text{O}_5$  an enhancement was observed by a modification of the electronic state of the Ir metal, accompanied by a reduction in the activation energy. In contrast to the activity, the selectivity (relative population of deuterioethanes) is affected by the nature of site II at the perimeter of the  $\text{NbO}_x$  island.

There may be two kinds of effects which the  $\text{NbO}_x$  island provides. One is a short-range effect which can exert an influence at only one or two atom distances from the periphery, and the other is a long-range effect which causes an electronic modification of the metal surface. The importance of short-range influences by the hetero-atom has been pointed out both experimentally and theoretically.<sup>26,27</sup> This influence may change the relative stability of the  $\pi$ - and  $\sigma$ -intermediates in the  $\text{D}_2$ -ethene reaction and suppress deuterium adsorption on metal atoms in the periphery of  $\text{NbO}_x$ . In contrast, the long-range effect may be weak, because no change in kinetic parameters was observed with LTR and HTR  $\text{Rh}/\text{Nb}_2\text{O}_5$  under the present conditions. For  $\text{Ir}/\text{Nb}_2\text{O}_5$  it was positive for hydrogen or deuterium dissociation, since the energy barrier for dissociation was reduced. The difference between Rh and Ir in the enhancement of  $\text{H}_2$ - $\text{D}_2$  exchange and ethene hydrogenation in the SMSI state may be of interest, but further investigation is necessary for its precise explanation. The phenomena observed on the  $\text{Rh}/\text{Nb}_2\text{O}_5$  and  $\text{Ir}/\text{Nb}_2\text{O}_5$  catalysts in the SMSI state may be more or less common to general metal catalysts with promoters.

## References

- 1 *Metal-Support and Metal-Additive Effects in Catalysis*, ed. B. Imelik, C. Naccache, G. Condurier, H. Praliaud, P. Meriaudeau, P. Gallezot, G. A. Martin and J. C. Vedrine (Elsevier, Amsterdam, 1982).
- 2 *Strong Metal-Support Interactions*, ed. R. T. K. Baker, S. J. Tauster and J. A. Dumesic, *Am. Chem. Symp. Ser. 298* (American Chemical Society, Washington, DC., 1986).
- 3 D. E. Resasco, R. J. Fenoglio, M. P. Suarez and J. O. Cechini, *J. Phys. Chem.*, 1986, **90**, 4330.
- 4 P. Meriaudeau, O. H. Ellestad, M. Dufaux and C. Naccache, *J. Catal.*, 1982, **75**, 243.
- 5 D. E. Resasco and G. L. Haller, *J. Catal.*, 1983, **82**, 279.
- 6 M. A. Vannice and R. L. Garten, *J. Catal.*, 1979, **56**, 236.
- 7 J. D. Bracy and K. Burch, *J. Catal.*, 1984, **78**, 389.
- 8 D. N. Benton, Y. M. Sun and J. M. White, *J. Am. Chem. Soc.*, 1984, **106**, 3059.
- 9 S. Takatani and Y. W. Chung, *J. Catal.*, 1984, **90**, 75.
- 10 H. R. Sadeghi and V. E. Henrich, *J. Catal.*, 1984, **87**, 279.
- 11 J. Santos, J. Philips and J. A. Dumesic, *J. Catal.*, 1983, **81**, 147.
- 12 X. Z. Jiang, T. F. Hayden and J. A. Dumesic, *J. Catal.*, 1983, **83**, 168.
- 13 M. A. Vannice and C. Sudhakar, *J. Phys. Chem.*, 1984, **88**, 2429.
- 14 J. D. Bracey and R. Burch, *J. Catal.*, 1984, **86**, 384.
- 15 W. M. H. Sachtler, D. F. Shriver, W. B. Hollenberg and A. F. Long, *J. Catal.*, 1985, **82**, 429.
- 16 G. C. Bond, *Catalysis by Metals* (Academic Press, London, 1962).
- 17 T. Keii, *J. Chem. Phys.*, 1954, **22**, 144.
- 18 C. Kemball, *J. Chem. Soc.*, 1956, 735.
- 19 G. C. Bond, J. J. Phillipson, P. B. Wells and J. M. Winterbottom, *Trans. Faraday Soc.*, 1964, **60**, 1847.
- 20 G. C. Bond, G. Webb, P. B. Wells and J. M. Winterbottom, *Trans. Faraday Soc.*, 1965, **61**, 1007.
- 21 B. A. Sexton, A. E. Hughes and K. Foger, *J. Catal.*, 1982, **77**, 85.
- 22 M. Nishimura, K. Asakura and Y. Iwasawa, *J. Chem. Soc., Chem. Commun.*, 1986, 1660; *Chem. Lett.*, 1987, 573.
- 23 H. Yoshitake, K. Asakura and Y. Iwasawa, unpublished data.
- 24 H. Yoshitake, K. Asakura and Y. Iwasawa, to be published.
- 25 (a) M. E. Levin, M. Salmeron, A. T. Bell and G. A. Somorjai, *J. Chem. Soc., Faraday Trans. 1*, 1987, **83**, 2061; (b) M. E. Levin, M. Salmeron, A. T. Bell and G. A. Somorjai, *J. Catal.*, 1987, **106**, 401.
- 26 J. M. Maclaren, J. B. Pendry, R. W. Joyner and P. Meehan, *Surf. Sci.*, 1986, **175**, 263.
- 27 J. M. Maclaren, J. B. Pendry and R. W. Joyner, *Surf. Sci.*, 1986, **178**, 856.

Paper 8/00212F; Received 19th January, 1988